Science AAAS

Kepler-62: A Five-Planet System with Planets of 1.4 and 1.6 Earth Radii in the Habitable Zone

William J. Borucki *et al.*

Science **340**, 587 (2013);
DOI: 10.1126/science.1234702

Small ion trap quantum simulators such as that reported here may soon reach this milestone with technical upgrades in the hardware, including lower vacuum chamber pressures to prevent collisions with the background gas, better stability of the optical intensities, and higher optical power so that fluctuations in the beam inhomogeneities can be suppressed.

References and Notes

1. H. T. Diep, *Frustrated Spin Systems* (World Scientific, Singapore, 2005).
2. R. Moessner, A. P. Ramirez, *Phys. Today* **59**, 24 (2006).
3. S. Sachdev, *Quantum Phase Transitions* (Cambridge Univ. Press, Cambridge, 1999).
4. R. Feynman, *Int. J. Theor. Phys.* **21**, 467 (1982).
5. I. Bloch, J. Dalibard, S. Nascimbéne, *Nat. Phys.* **8**, 267 (2012).
6. R. Blatt, C. F. Roos, *Nat. Phys.* **8**, 277 (2012).
7. J. Simon *et al.*, *Nature* **472**, 307 (2011).
8. G.-B. Jo *et al.*, *Phys. Rev. Lett.* **108**, 045305 (2012).
9. D. Porras, J. I. Cirac, *Phys. Rev. Lett.* **92**, 207901 (2004).
10. A. Friedenauer, H. Schmitz, J. T. Glueckert, D. Porras, T. Schaetz, *Nat. Phys.* **4**, 757 (2008).
11. K. Kim *et al.*, *Phys. Rev. Lett.* **103**, 120502 (2009).
12. R. Islam *et al.*, *Nat. Commun.* **2**, 377 (2011).
13. J. W. Britton *et al.*, *Nature* **484**, 489 (2012).
14. A. Khromova *et al.*, *Phys. Rev. Lett.* **108**, 220502 (2012).
15. K. Kim *et al.*, *Nature* **465**, 590 (2010).
16. E. E. Edwards *et al.*, *Phys. Rev. B* **82**, 060412 (2010).
17. S. Olmschenk *et al.*, *Phys. Rev. A* **76**, 052314 (2007).
18. See supplementary materials on *Science* Online.
19. K. Binder, *Phys. Rev. Lett.* **47**, 693 (1981).
20. C. Shen, L.-M. Duan, *New J. Phys.* **14**, 053053 (2012).
21. W. C. Campbell *et al.*, *Phys. Rev. Lett.* **105**, 090502 (2010).
22. C.-C. J. Wang, J. K. Freericks, *Phys. Rev. A* **86**, 032329 (2012).
23. R. Moessner, S. L. Sondhi, *Phys. Rev. B* **63**, 224401 (2001).
24. A. W. Sandvik, *Phys. Rev. Lett.* **104**, 137204 (2010).
25. Quantum Monte Carlo algorithms can be used to calculate static equilibrium properties of the transverse field Ising model for large numbers of interacting spins, so ground states and static correlation functions can indeed be calculated for large systems (*23*). However, the calculation of dynamics and nonequilibrium behavior of quantum spin models is not currently feasible for these Monte Carlo approaches, and in the presence of frustrated long-range interactions, the general behavior of such systems requires exact diagonalization. Other techniques such as the density matrix renormalization group become too difficult with long-range interactions. Because the size of the Hilbert space grows exponentially with the number of spins, sparse-matrix techniques such as the Lanczos method must therefore be used. Current state-of-the-art work on such systems is limited to sizes on the order of 30 to 35 spins (*24*).

Acknowledgments: We thank E. Demler, L. Duan, D. Huse, K. Kim, P. Richerme, R. Sensarma, and P. Zoller for critical discussions. This work is supported by the U.S. Army Research Office (ARO) award W911NF0710576 with funds from the Defense Advanced Research Projects Agency Optical Lattice Emulator Program, ARO award W911NF0410234 with funds from the Intelligence Advanced Research Projects Activity, and the NSF Physics Frontier Center at the Joint Quantum Institute. J.K.F. was also supported by the McDevitt bequest at Georgetown.

Supplementary Materials
www.sciencemag.org/cgi/content/full/340/6132/583/DC1
Supplementary Text
Fig. S1
References (*26–28*)

2 November 2012; accepted 8 February 2013
10.1126/science.1232296

Kepler-62: A Five-Planet System with Planets of 1.4 and 1.6 Earth Radii in the Habitable Zone

William J. Borucki,[1,*] Eric Agol,[2] Francois Fressin,[3] Lisa Kaltenegger,[3,4] Jason Rowe,[5] Howard Isaacson,[6] Debra Fischer,[7] Natalie Batalha,[1] Jack J. Lissauer,[1] Geoffrey W. Marcy,[6] Daniel Fabrycky,[8,9] Jean-Michel Désert,[3] Stephen T. Bryson,[1] Thomas Barclay,[10] Fabienne Bastien,[11] Alan Boss,[12] Erik Brugamyer,[13] Lars A. Buchhave,[14,15] Chris Burke,[5] Douglas A. Caldwell,[5] Josh Carter,[3] David Charbonneau,[3] Justin R. Crepp,[16,17] Jørgen Christensen-Dalsgaard,[18] Jessie L. Christiansen,[5] David Ciardi,[19] William D. Cochran,[13] Edna DeVore,[5] Laurance Doyle,[5] Andrea K. Dupree,[3] Michael Endl,[13] Mark E. Everett,[20] Eric B. Ford,[21] Jonathan Fortney,[8] Thomas N. Gautier III,[22] John C. Geary,[3] Alan Gould,[23] Michael Haas,[1] Christopher Henze,[1] Andrew W. Howard,[24] Steve B. Howell,[1] Daniel Huber,[1] Jon M. Jenkins,[5] Hans Kjeldsen,[18] Rea Kolbl,[6] Jeffery Kolodziejczak,[25] David W. Latham,[3] Brian L. Lee,[2] Eric Lopez,[8] Fergal Mullally,[5] Jerome A. Orosz,[26] Andrej Prsa,[27] Elisa V. Quintana,[5] Roberto Sanchis-Ojeda,[30] Dimitar Sasselov,[3] Shawn Seader,[5] Avi Shporer,[8,28] Jason H. Steffen,[29] Martin Still,[10] Peter Tenenbaum,[5] Susan E. Thompson,[5] Guillermo Torres,[3] Joseph D. Twicken,[5] William F. Welsh,[26] Joshua N. Winn[30]

We present the detection of five planets—Kepler-62b, c, d, e, and f—of size 1.31, 0.54, 1.95, 1.61 and 1.41 Earth radii ($R_\oplus$), orbiting a K2V star at periods of 5.7, 12.4, 18.2, 122.4, and 267.3 days, respectively. The outermost planets, Kepler-62e and -62f, are super–Earth-size (1.25 $R_\oplus$ < planet radius ≤ 2.0 $R_\oplus$) planets in the habitable zone of their host star, respectively receiving 1.2 ± 0.2 times and 0.41 ± 0.05 times the solar flux at Earth's orbit. Theoretical models of Kepler-62e and -62f for a stellar age of ~7 billion years suggest that both planets could be solid, either with a rocky composition or composed of mostly solid water in their bulk.

Kepler is a NASA Discovery-class mission designed to determine the frequency of Earth-radius planets in and near the habitable zone (HZ) of solar-like stars (*1–6*). Planets are detected as "transits" that cause the host star to appear periodically fainter when the planets pass in front of it along the observer's line of sight. Kepler-62 [Kepler Input Catalog (KIC) 9002278, Kepler Object of Interest (KOI) 701] is one of about 170,000 stars observed by the Kepler spacecraft. On the basis of an analysis of long-cadence photometric observations from Kepler taken in quarters 1 through 12 (13 May 2009 through 28 March 2012), we report the detection of five planets orbiting Kepler-62, including two super–Earth-size planets in the HZ as well as a hot Mars-size planet (Fig. 1 and Table 1). Before validation, three of these objects were designated as planetary candidates KOI-701.01, 701.02, and 701.03 in the Kepler 2011 catalog (*7*) and the Kepler 2012 catalog (*8*). KOI-701.04 and 701.05 were subsequently identified using a larger data sample (*9*).

Analysis of high-resolution spectra indicates that Kepler-62 is a K2V spectral type with an estimated mass and radius (in solar units) of 0.69 ± 0.02 $M_\odot$ and 0.63 ± 0.02 $R_\odot$ (*9*). Examination of the sky close to Kepler-62 showed the presence of only one additional star that contributed as much as 1% to the total flux (figs. S3 and S4) (*9*). Warm-Spitzer observations (fig. S9) and the analysis of centroid motion (table S1) were consistent with the target star as the source of the transit signals (Fig. 1 and fig. S1). We computed the radius, semimajor axis, and radiative equilibrium temperature of each planet (Table 1) on the basis of light curve modeling given the derived stellar parameters (table S3).

The masses of the planets could not be directly determined using radial velocity (RV) measurements of the host star because of the planets' low masses, the faintness and variability of the star, and the level of instrument noise. In the absence of a detected signal in the RV measurements (*9*), we statistically validated the planetary nature of Kepler-62b through -62f with the BLENDER procedure (*10–13*) by comparing the probability of eclipsing binaries and other false-positive scenarios to bona fide transiting planet signals (*14–18*).

To systematically explore the different types of false positives that can mimic the signals, we generated large numbers of synthetic light curves that blend together light from multiple stars and planets over a wide range of parameters, and then compared each blend with the Kepler photometry (Fig. 2). We rejected blends that resulted in light curves inconsistent with the observations.

We then estimated the frequency of the allowed blends by taking into account all available observational constraints from the follow-up observations discussed in (*9*). Finally, we compared this frequency with the expected frequency of true planets (planet "prior") to derive the odds ratio (*9*). By incorporating these constraints into a Monte Carlo model that considered a wide range of stellar and planetary characteristics, we determined estimates of the probability of each false positive that could explain the observations (*9*).

Our simulations of each of the candidates indicate that the likelihood of a false-positive explanation is much smaller than the likelihood that the candidates constitute a planetary system. The calculated odds ratios that Kepler-62b through -62f represent planets rather than false positives are 5400, >5000, 15,000, 14,700, and >5000, respectively (*9*). There is also a 0.2% chance that the planets orbit a widely spaced binary composed of two K2V stars; if so, the planets are larger in radius than the values shown in Table 1 by a factor of $\sqrt{2}$ (*9*).

To determine whether a planet is in the HZ, we calculated the flux of stellar radiation that it intercepts. It is convenient to express intercepted flux in units of the average solar flux intercepted by Earth, denoted by $S_\odot$. The values of the stellar flux intercepted by Kepler-62b to -62f are $70 \pm 9\ S_\odot$, $25 \pm 3\ S_\odot$, $15 \pm 2\ S_\odot$, $1.2 \pm 0.2\ S_\odot$, and $0.41 \pm 0.05\ S_\odot$, respectively. Eccentric planetary orbits increase the annually averaged irradiation from the primary star by a factor of $1/(1 - e^2)^{1/2}$, where e is the orbital eccentricity (*19*). Because the model results for the orbital eccentricities of Kepler-62b through -62f are small and consistent with zero, no corrections were made.

The HZ is defined here as the annulus around a star where a rocky planet with a CO_2-H_2O-N_2 atmosphere and sufficiently large water content (such as on Earth) can host liquid water on its solid surface (*20*). In this model, the locations of the two edges of the HZ are determined on the basis of the stellar flux intercepted by the planet and the assumed composition of the atmosphere. A conservative estimate of the range of the HZ (labeled "narrow HZ" in Fig. 3) is derived from atmospheric models by assuming that the planets have H_2O- and CO_2-dominated atmospheres with no cloud feedback (*21*). The flux range is defined at the inner edge by thermal runaway due to saturation of the atmosphere by water vapor and at the outer edge by the freeze-out of CO_2. In this model, the planets are assumed to be geologically active and climatic stability is provided by a mechanism in which atmospheric CO_2 concentration varies inversely with planetary surface temperature.

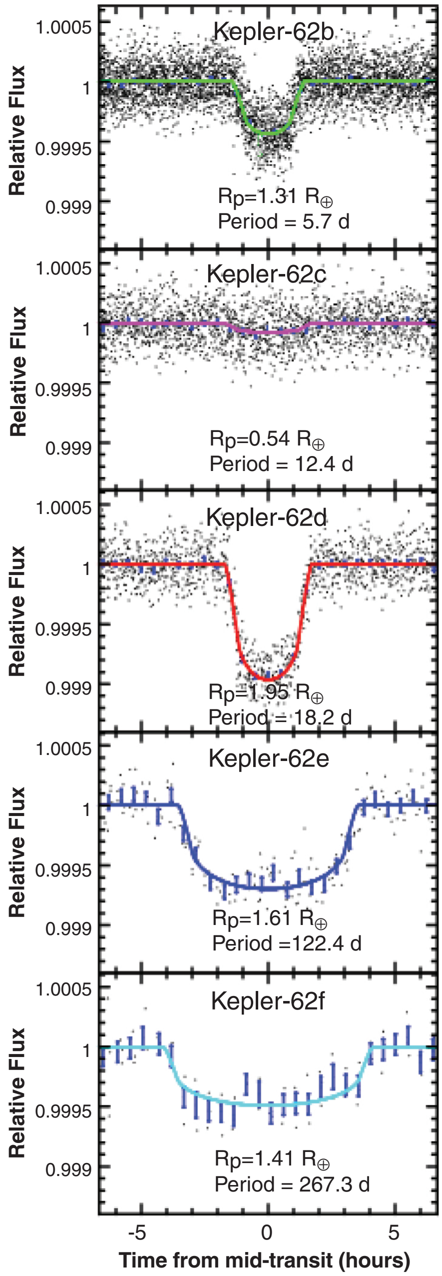

Fig. 1. Kepler-62 light curves after the data were detrended to remove the stellar variability. Composite of phase-folded transit light curves (dots), data binned in ½ hour intervals (blue error bars), and model fits (colored curves) for Kepler-62b through -62f. Model parameters are provided in Table 1. The error bars get larger as the period becomes larger because there are fewer points to bin together. For the shortest periods, the bars are too small to see.

The "empirical" HZ boundaries are defined by the solar flux received at the orbits of Venus and Mars at the epochs when they potentially had liquid water on their surfaces. Venus and Mars are believed to have lost their water at least 1 billion years and 3.8 billion years ago, respectively, when the Sun was less luminous. At these epochs, Venus received a flux of 1.78 $S_\odot$ and Mars a flux of 0.32 $S_\odot$ (*20*). The stellar spectral energy distributions of stars cooler than the Sun are expected to slightly increase the absorbed flux (*20*). Including this factor changes the HZ flux limits to 1.66 and 0.27 $S_\odot$ for the empirical HZ, and 0.95 and 0.29 $S_\odot$ for the narrow HZ (*21*). Figure 3 shows that Earth and Kepler-62f are within the flux boundaries of the narrow HZ, whereas Kepler-22b and Kepler-62e are within the empirical flux boundaries.

Although RV observations were not precise enough to measure masses for Kepler-62e and -62f, other exoplanets with a measured radius below 1.6 $R_\oplus$ have been found to have densities indicative of a rocky composition. In particular, Kepler-10b (*22*), Kepler-36b (*23*), and CoRoT-7b (*24*) have radii of 1.42 $R_\oplus$, 1.49 $R_\oplus$, and 1.58 $R_\oplus$ and densities of 8.8, 7.5, and 10.4 g/cm^3, respectively. Thus, it is possible that both Kepler-62e and -62f (with radii of 1.61 $R_\oplus$ and 1.41 $R_\oplus$) are also rocky planets.

The albedo and the atmospheric characteristics of these planets are unknown, and therefore the range of equilibrium temperatures (T_{eq}) at which the thermal radiation from each planet balances the insolation is large and depends strongly on the composition and circulation of the planets' atmospheres, their cloud characteristics and coverage, and the planets' rotation rates (*25*, *26*). However, for completeness, values of T_{eq} were computed from $T_{eq} = T_{eff}[\beta(1 - A_B)(R_*/2a)^2]^{1/4}$, where T_{eff} is the effective temperature of the star (4925 K), R_* is the radius of the star relative to the Sun (0.64), A_B is the planet Bond albedo, a is the planet semimajor axis, and β is a proxy for day-night redistribution (1 = full redistribution, 2 = no redistribution). For the Markov chain Monte Carlo calculations, it was assumed that β = 1 and that A_B is a random number from 0 to 0.5 (Table 1).

[1]NASA Ames Research Center, Moffett Field, CA 94035, USA. [2]Department of Astronomy, Box 351580, University of Washington, Seattle, WA 98195, USA. [3]Harvard-Smithsonian Center for Astrophysics, Cambridge, MA 02138, USA. [4]Max Planck Institute of Astronomy, Koenigstuhl 17, 69115 Heidelberg, Germany. [5]SETI Institute, Mountain View, CA 94043, USA. [6]University of California, Berkeley, CA 94720, USA. [7]Yale University, New Haven, CT 06520, USA. [8]Department of Astronomy and Astrophysics, University of California, Santa Cruz, CA 95064, USA. [9]Department of Astronomy and Astrophysics, University of Chicago, Chicago, IL 60637, USA. [10]Bay Area Environmental Research Institute, Moffett Field, CA 94035, USA. [11]Vanderbilt University, Nashville, TN 37235, USA. [12]Carnegie Institution of Washington, Washington, DC 20015, USA. [13]McDonald Observatory, University of Texas, Austin, TX 78712, USA. [14]Niels Bohr Institute, University of Copenhagen, DK-2100 Copenhagen, Denmark. [15]Centre for Star and Planet Formation, Natural History Museum of Denmark, University of Copenhagen, DK-1350 Copenhagen, Denmark. [16]Department of Astronomy, California Institute of Technology, Pasadena, CA 91125, USA. [17]Department of Physics, University of Notre Dame, Notre Dame, IN 46556, USA. [18]Department of Physics and Astronomy, Aarhus University, Aarhus, Denmark. [19]Exoplanet Science Institute/Caltech, Pasadena, CA 91125, USA. [20]National Optical Astronomy Observatory, Tucson, AZ 85719, USA. [21]University of Florida, Gainesville, FL 32611, USA. [22]Jet Propulsion Laboratory, California Institute of Technology, Pasadena, CA 91109, USA. [23]Lawrence Hall of Science, Berkeley, CA 94720, USA. [24]Institute for Astronomy, University of Hawaii, Honolulu, HI 96822, USA. [25]Marshall Space Flight Center, Huntsville, AL 35805, USA. [26]San Diego State University, San Diego, CA 92182, USA. [27]Villanova University, Villanova, PA 19085, USA. [28]Las Cumbres Observatory Global Telescope, Goleta, CA 93117, USA. [29]Northwestern University, Evanston, IL 60208, USA. [30]Massachusetts Institute of Technology, Cambridge, MA 02139, USA.

*Corresponding author. E-mail: william.j.borucki@nasa.gov

Gravitational interactions between Kepler-62e and -62f are too weak (*9*) to cause nonlinear variations in the times of transits (*27*, *28*) and thereby provide estimates of their masses. Nevertheless, upper limits (95th percentile) for Kepler-62e and -62f were derived (table S4): 150 $M_\oplus$ and 35 $M_\oplus$, respectively. The smallest upper limit to the mass of Kepler-62e based on RV observations (table S4) gives 36 $M_\oplus$. These values confirm their planetary nature without constraining their composition. Despite the lack of a measured mass for Kepler-62e and -62f, the precise knowledge of their radii, combined with estimates of their T_{eq} and the stellar age (~7 billion years), imply that Kepler-62e and -62f have lost their primordial or outgassed hydrogen envelope (*29*, *30*). Therefore, Kepler-62e and -62f are Kepler's first HZ planets that could plausibly be composed of

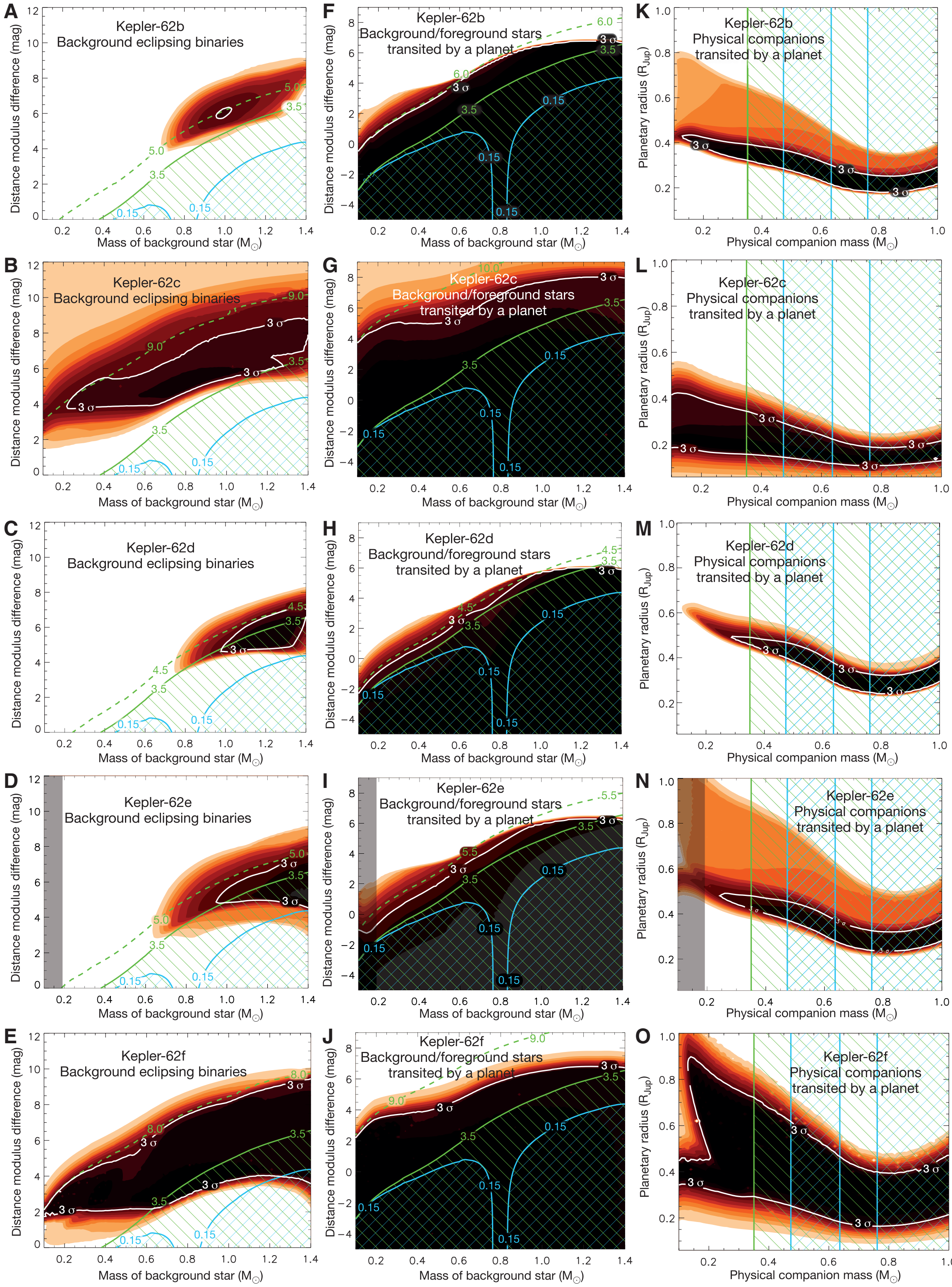

Fig. 2. BLENDER goodness-of-fit contours for Kepler-62b, c, d, e, and f corresponding to the three different scenarios that contribute to the overall blend frequency. (**A** to **E**) Background eclipsing binaries. (**F** to **J**) Background or foreground stars transited by a planet. (**K** to **O**) Physical companions transited by a planet. Viable blends must be less than ~5.0 magnitudes [(A) to (E)] or ~5.5 magnitudes [(F) to (J)] fainter than Kepler-62 (dashed line). Only blends inside the solid white contour match the Kepler light curve within acceptable limits (3σ, where σ is the significance level of the χ^2 difference compared to a transit model fit). Lighter-colored areas (red, orange, yellow) mark regions of parameter space giving increasingly worse fits to the data (4σ, 5σ, etc.) and correspond to blends that we consider to be ruled out. The cyan cross-hatched areas indicate regions of parameter space that we have ruled out because the resulting r-Ks color of the blend is either too red (left) or too blue (right), relative to the measured color, by more than 3σ (0.15 mag). The green hatched regions indicate blends that are ruled out because the intruding stars are less than 3.5 magnitudes fainter than the target and would be so bright that they would have been detected spectroscopically. Finally, the thin gray area at the left of (D), (I), and (N) rules out stars on the basis of our Spitzer observations (fig. S8) (*9*). The likelihood of a false positive for each planetary candidate is derived from the integration of the area that remains within the 3σ boundary that is not eliminated by the hatched areas.

Table 1. Characteristics of the Kepler-62 planetary system. T_0 is the epoch in mid-transit in barycentric Julian days, P is the period, "depth" is the percent reduction of the flux during the transits determined from the model fit to the data, R_p/R_* is the ratio of the radius of the planet to the radius of the star, a/R_* is the ratio of the planet's semimajor axis to the stellar radius, b is the impact parameter in units of stellar radius, i is the orbital inclination, $e \cos \omega$ is the product of the orbital eccentricity e and the cosine of the periapse angle ω, a is the planet semimajor axis, R_p is the planet radius, maximum mass is the upper limit to the mass based on transiting timing and RV observations, $M_\oplus$ is the mass of Earth, and T_{eq} is the radiative equilibrium temperature. The values of the uncertainties are ±1 standard deviation unless otherwise noted. Values for the maximum mass are for the 95th percentile (*9*). A second set of values for the planetary parameters was computed by an independent model and found to be in good agreement with the listed values.

Parameter	Kepler-62b	Kepler-62c	Kepler-62d	Kepler-62e	Kepler-62f
T_0 (BJD-2454900)	103.9189 ± 0.0009	67.651 ± 0.008	113.8117 ± 0.0008	83.404 ± 0.003	522.710 ± 0.006
P (days)	5.714932 ± 0.000009	12.4417 ± 0.0001	18.16406 ± 0.00002	122.3874 ± 0.0008	267.291 ± 0.005
Transit duration (hours)	2.31 ± 0.09	3.02 ± 0.09	2.97 ± 0.09	6.92 ± 0.16	7.46 ± 0.20
Depth (%)	0.043 ± 0.001	0.007 ± 0.001	0.092 ± 0.002	0.070 ± 0.003	0.042 ± 0.004
R_p/R_*	0.0188 ± 0.0003	0.0077 ± 0.0004	0.0278 ± 0.0006	0.0232 ± 0.0003	0.0203 ± 0.0008
a/R_*	18.7 ± 0.5	31.4 ± 0.8	40.4 ± 1.0	144 ± 4	243 ± 6
b	0.25 ± 0.13	0.16 ± 0.09	0.22 ± 0.13	0.06 ± 0.05	0.41 ± 0.14
i	89.2 ± 0.4	89.7 ± 0.2	89.7 ± 0.3	89.98 ± 0.02	89.90 ± 0.03
$e \cos \omega$	0.01 ± 0.17	–0.05 ± 0.14	–0.03 ± 0.24	0.05 ± 0.17	–0.05 ± 0.14
$e \sin \omega$	–0.07 ± 0.06	–0.18 ± 0.11	0.09 ± 0.09	–0.12 ± 0.02	–0.08 ± 0.10
a (AU)	0.0553 ± 0.0005	0.0929 ± 0.0009	0.120 ± 0.001	0.427 ± 0.004	0.718 ± 0.007
R_p ($R_\oplus$)	1.31 ± 0.04	0.54 ± 0.03	1.95 ± 0.07	1.61 ± 0.05	1.41 ± 0.07
Maximum mass ($M_\oplus$) (*9*)	9	4	14	36	35
Number of observed transits	171	76	52	8	3
Total SNR	54	8.5	68	31	12
T_{eq} (K)	750 ± 41	578 ± 31	510 ± 28	270 ± 15	208 ± 11

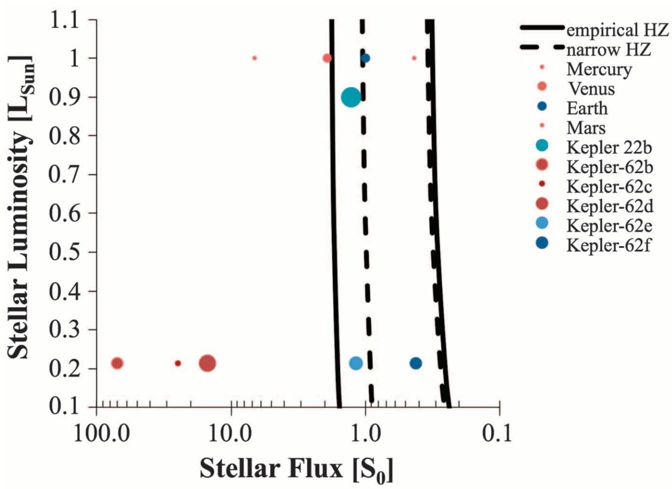

Fig. 3. Comparison of known HZ exoplanets with measured radii less than 2.5 $R_\oplus$ to the solar system planets. The sizes of the circles indicate the relative sizes of the planets to each other. The dashed and solid lines indicate the edges of the narrow and empirical HZ, respectively.

condensable compounds and be solid, either as a dry, rocky super-Earth or composed of a substantial amount of water (most of which would be in a solid phase because of the high internal pressure) surrounding a silicate-iron core.

We do not know whether Kepler-62e and -62f have a rocky composition, an atmosphere, or water. Until we get suitable spectra of their atmospheres, we cannot determine whether they are in fact habitable. With radii of 1.61 and 1.41 $R_\oplus$, respectively, Kepler-62e and -62f are the smallest transiting planets detected by the Kepler mission that orbit within the HZ of any star other than the Sun.

References and Notes

1. W. Borucki *et al.*, *Proc. IAU* **4**, S253 (2009).
2. N. M. Batalha *et al.*, *Astrophys. J.* **713**, L109 (2010).
3. D. G. Koch *et al.*, *Astrophys. J.* **713**, L79 (2010).
4. V. S. Argabright *et al.*, *Proc. SPIE* **7010**, 70102L (2008).
5. W. J. Borucki *et al.*, *Science* **327**, 977 (2010).
6. J. M. Jenkins *et al.*, *Astrophys. J.* **713**, L87 (2010).
7. W. J. Borucki *et al.*, *Astrophys. J.* **736**, 19 (2011).
8. N. M. Batalha *et al.*, http://arxiv.org/abs/1202.5852 (2012).
9. See supplementary materials on *Science* Online.
10. G. Torres, M. Konacki, D. D. Sasselov, S. Jha, *Astrophys. J.* **614**, 979 (2004).
11. G. Torres *et al.*, *Astrophys. J.* **700**, 1589 (2011).
12. F. Fressin *et al.*, *Astrophys. J. Suppl. Ser.* **197**, 5 (2011).
13. F. Fressin *et al.*, *Nature* **482**, 195 (2012).
14. J. M. Désert *et al.*, *Astron. Astrophys.* **526**, A12 (2011).
15. S. Ballard *et al.*, *Astrophys. J.* **743**, 200 (2011).
16. W. J. Borucki *et al.*, *Astrophys. J.* **745**, 120 (2012).
17. S. Howell *et al.*, *Astrophys. J.* **746**, 123 (2012).
18. T. N. Gautier III *et al.*, *Astrophys. J.* **749**, 15 (2012).
19. D. M. Williams, D. Pollard, *Int. J. Astrobiol.* **1**, 61 (2002).
20. J. F. Kasting, D. P. Whitmire, R. T. Reynolds, *Icarus* **101**, 108 (1993).
21. R. K. Kopparapu *et al.*, http://arxiv.org/abs/1301.6674 (2013).
22. N. M. Batalha *et al.*, *Astrophys. J.* **729**, 27 (2011).
23. J. A. Carter *et al.*, *Science* **337**, 556 (2012).
24. A. P. Hatzes *et al.*, *Astrophys. J.* **743**, 75 (2011).
25. F. Selsis *et al.*, *Astron. Astrophys.* **476**, 1373 (2007).
26. L. Kaltenegger, D. Sasselov, *Astrophys. J.* **736**, L25 (2011).
27. M. J. Holman, N. W. Murray, *Science* **307**, 1288 (2005).
28. E. Agol, J. Steffen, R. Sari, W. Clarkson, *Mon. Not. R. Astron. Soc.* **359**, 567 (2005).
29. L. Rogers, S. Seager, *Astrophys. J.* **716**, 1208 (2010).
30. E. D. Lopez, J. J. Fortney, N. K. Miller, http://arxiv.org/abs/1205.0010 (2012).

Acknowledgments: Kepler was competitively selected as the 10th Discovery mission. Funding for this mission is provided by NASA's Science Mission Directorate. Some of the data presented herein were obtained at the W. M. Keck Observatory, which is operated as a scientific partnership of the California Institute of Technology, the University of California, and NASA. The Keck Observatory was made possible by the generous financial support of the W. M. Keck Foundation. L.K. acknowledges support from Deutsche Forschungsgemeinschaft grants ENP Ka 3142/1-1 and NASA Astrobiology Institute. Funding for the Stellar Astrophysics Centre is provided by the Danish National Research Foundation. The research is supported by the ASTERISK project (Asteroseismic Investigations with SONG and Kepler) funded by European Research Council grant 267864. W.F.W. and J.A.O. acknowledge support from NASA through the Kepler Participating Scientist Program (PSP) and from NSF grant AST-1109928. D.F. acknowledges support from NASA ADAP12-0172. O.R.S.-O. and J.N.W. are supported by the Kepler PSP through grant NNX12AC76G. E.F. is partially supported by NASA PSP grants NNX08AR04G and NNX12AF73G. E.A. acknowledges NSF career grant AST-0645416. We also thank the Spitzer staff at IPAC and in particular N. Silbermann for checking and scheduling the Spitzer observations. The Spitzer Space Telescope is operated by the Jet Propulsion Laboratory, California Institute of Technology, under a contract with NASA. We thank the many people who gave so generously of their time to make this mission a success. All data products are available to the public at the Mikulski Archive for Space Telescopes, http://stdatu.stsci.edu/kepler.

Supplementary Materials

www.sciencemag.org/cgi/content/full/science.1234702/DC1
Materials and Methods
Supplementary Text
Figs. S1 to S14
Tables S1 to S4
References (*31–57*)

2 January 2013; accepted 5 April 2013
Published online 18 April 2013;
10.1126/science.1234702